Single mode operation with mid-IR hollow fibers in the range 5.1-10.5 µm

Angelo Sampaolo,[1,2] Pietro Patimisco,[1,2] Jason M. Kriesel,[3] Frank K. Tittel,[2] Gaetano Scamarcio,[1] and Vincenzo Spagnolo[1*]

[1]*Dipartimento Interateneo di Fisica, Università e Politecnico di Bari, CNR-IFN UOS BARI, Via Amendola 173, Bari, Italy*
[2]*Department of Electrical and Computer Engineering, Rice University, 6100 Main Street, Houston, TX 77005, USA*
[3]*Opto-Knowledge Systems, Inc. (OKSI), 19805 Hamilton Ave., Torrance CA, USA 90502-1341, USA*
[*]*vincenzo.spagnolo@uniba.it*

Abstract: Single mode beam delivery in the mid-infrared spectral range 5.1-10.5 µm employing flexible hollow glass waveguides of 15 cm and 50 cm lengths, with metallic/dielectric internal layers and a bore diameter of 200 µm were demonstrated. Three quantum cascade lasers were coupled with the hollow core fibers. For a fiber length of 15 cm, we measured losses down to 1.55 dB at 5.4 µm and 0.9 dB at 10.5 µm. The influence of the launch conditions in the fiber on the propagation losses and on the beam profile at the waveguide exit was analyzed. At 10.5 µm laser wavelength we found near perfect agreement between measured and theoretical losses, while at ~5 µm and ~6 µm wavelengths the losses were higher than expected. This discrepancy can be explained considering an additional scattering loss effect, which scales as $1/\lambda^2$ and is due to surface roughness of the metallic layer used to form the high-reflective internal layer structure of the hollow core waveguide.

OCIS codes: (060.2390) Fiber optics, infrared; (140.5965) Semiconductor lasers, quantum cascade.

References and links

1. B. Lendl and B. Mizaikoff, *Optical Fibers for Mid-infrared Spectrometry, Handbook of Vibrational Spectroscopy Vol. 2* (John Wiley & Sons Ltd, 2002).
2. J. A. Harrington, "A review of IR transmitting, hollow waveguides," Fiber and Integrated Opt. **19**(3), 211–227 (2000).
3. V. Spagnolo, P. Patimisco, S. Borri, G. Scamarcio, B. E. Bernacki, and J. Kriesel, "Mid-infrared fiber-coupled QCL-QEPAS sensor," Appl. Phys. B **112**(1), 25–33 (2013).
4. V. Spagnolo, P. Patimisco, S. Borri, G. Scamarcio, B. E. Bernacki, and J. Kriesel, "Part-per-trillion level SF_6 detection using a quartz enhanced photoacoustic spectroscopy-based sensor with single-mode fiber-coupled quantum cascade laser excitation," Opt. Lett. **37**(21), 4461–4463 (2012).
5. J. A. Harrington, *Infrared Fibers and Their Applications* (SPIE, 2004).
6. C. M. Bledt, J. A. Harrington, and J. M. Kriesel, "Loss and modal properties of Ag/AgI hollow glass waveguides," Appl. Opt. **51**(16), 3114–3119 (2012).
7. P. Patimisco, V. Spagnolo, M. S. Vitiello, A. Tredicucci, G. Scamarcio, C. M. Bledt, and J. A. Harrington, "Coupling external cavity mid-IR quantum cascade lasers with low loss hollow metallic/dielectric waveguides," Appl. Phys. B **108**(2), 255–260 (2012).
8. P. Patimisco, V. Spagnolo, M. S. Vitiello, G. Scamarcio, C. M. Bledt, J. A. Harrington, and J. A. Harrington, "Low-loss hollow waveguide fibers for mid-infrared quantum cascade laser sensing applications," Sensors (Basel) **13**(1), 1329–1340 (2013).
9. R. Nubling and J. A. Harrington, "Launch conditions and mode coupling in hollow glass waveguides," Opt. Eng. **37**(9), 2454–2458 (1998).
10. J. Kriesel, G. M. Hagglund, N. Gat, V. Spagnolo, and P. Patimisco, "Spatial mode filtering of mid-infrared (mid-IR) laser beams with hollow core fiber optics," Proc. SPIE **8993**, 89930V (2014).
11. https://www.thorlabs.com/newgrouppage9.cfm?objectgroup_id=7062#SingleMode.
12. C. Caillaud, G. Renversez, L. Brilland, D. Mechin, L. Calvez, J.-L. Adam, and J. Troles, "Photonic bandgap propagation in all-solid chalcogenide microstructured optical fibers," Materials **7**(9), 6120–6129 (2014).

13. M. Siciliani de Cumis, S. Viciani, S. Borri, P. Patimisco, A. Sampaolo, G. Scamarcio, P. De Natale, F. D'Amato, and V. Spagnolo, "Widely-tunable mid-infrared fiber-coupled quartz-enhanced photoacoustic sensor for environmental monitoring," Opt. Express **22**(23), 28222–28231 (2014).
14. R. L. Kozodoy, A. T. Pagkalinawan, and J. A. Harrington, "Small-bore hollow waveguides for delivery of 3-μm laser radiation," Appl. Opt. **35**(7), 1077–1082 (1996).
15. Y. Matsuura, T. Abel, and J. A. Harrington, "Optical properties of small-bore hollow glass waveguides," Appl. Opt. **34**(30), 6842–6847 (1995).
16. R. S. Quimby, *Photonics and Lasers: An Introduction* (John Wiley & Sons Ltd, 2006).
17. E. A. J. Marcantili and R. A. Schmeltzer, "Hollow metallic and dielectric waveguides for long distance optical transmission and lasers," Bell Syst. Tech. J. **43**(4), 1783–1809 (1964).
18. Y. Matsuura and M. Miyagi, "Hollow optical fibers for ultraviolet and vacuum ultraviolet light," IEEE J. Sel. Top. Quant. **10**(6), 1430–1434 (2004).
19. C. Dragone, "Attenuation and radiation characteristics of the HE_{11} mode," IEEE T. Microw. Theory **28**(7), 704–710 (1980).
20. M. Miyagi and S. Kawakami, "Design theory of dielectric-coated circular metallic waveguides for infrared transmission," J. Lightwave Technol. **2**(2), 116–126 (1984).
21. R. George and J. A. Harrington, "Infrared transmissive, hollow plastic waveguides with inner Ag-Agl coatings," Appl. Opt. **44**(30), 6449–6455 (2005).
22. Y. Matsuura, M. Saito, M. Miyagi, and A. Hongo, "Loss characteristics of circular hollow waveguides for incoherent infrared light," J. Opt. Soc. Am. A **6**(3), 423–427 (1989).
23. C. D. Rabii, D. J. Gibson, and J. A. Harrington, "Processing and characterization of silver films used to fabricate hollow glass waveguides," Appl. Opt. **38**(21), 4486–4493 (1999).
24. M. Miyagi, "Bending losses in hollow and dielectric tube leaky waveguides," Appl. Opt. **20**(7), 1221–1229 (1981).

1. Introduction

Hollow-core waveguides (HCWs) are excellent for the transmission of infrared laser radiation, as they offer good flexibility for easy handling and high output beam quality for precise medical applications. Potential uses include not only laser surgery, but also numerous applications in infrared spectroscopy, thermal imaging, sensing and infrared countermeasures [1–4]. The HCWs structure is composed of a hollow glass capillary tube with a metallic/dielectric structure deposited inside the bore [5]. The bore size, typically < 1 mm, determines the overall losses and mode quality of the HCW, whereas the thickness of the dielectric layer determines the spectral response [6]. HCWs have extremely high coupling efficiency (e.g., > 95%), no back reflection, no cladding modes, and high energy/power handling capabilities [5, 7, 8]. An additional important feature of hollow waveguides is that despite the relatively large bore size, they can be quasi single mode. This is the result of the strong dependence of loss on the fiber mode parameters [5, 6, 9]. The single mode propagation and mode filtering capabilities have been found to depend strongly on the fiber diameter and the laser wavelength. Low-loss single mode propagation and effective mode filtering have been successfully demonstrated for HCWs with bore diameters of 300 μm with $\lambda > 8$ μm [3, 4, 10]. Note also that, single mode operation has been achieved with solid core fibers for $\lambda \leq 5.5$ μm (although the optical losses becomes very high for $\lambda > 4{,}6$ μm) [11] and with photonic band-gap fibers made by chalcogenide glasses at 3.39 μm, 9.3 μm, and 10.6 μm [12]. Empirically, hollow core fibers with bore sizes as large as 40 times the wavelength have been shown to provide a convenient, relatively low-loss means of delivering mid-IR laser beams with a single spatial mode. Consequently, HCWs with bore sizes up to 200 μm can operate in single mode when light at wavelength > 5 μm is guided inside, although until now this has been demonstrated only for $\lambda \geq 7.6$ μm [13].

In this paper, we demonstrated HCW single mode performance at wavelengths down to $\lambda = 5.1$ μm. The fiber realized for this work has a bore diameter of 200 μm and lengths of 15 cm and 50 cm. Three commercial mid-IR external cavity quantum cascade laser (QCL) sources with spectral ranges of emission centered at 5.2 μm, 6 μm and 10 μm were employed. Different coupling conditions between the lasers beam and the waveguides entrance were investigated using mid-infrared ZnSe, Ge, or CaF_2 lenses with focal lengths in the range 25-76 mm. The mode quality of the output beam and the propagation losses are highly dependent on the beam waist of the coupling lens. The measured HCW losses are slightly higher than the calculated values. These differences are larger for 5-6 μm wavelengths (up to ~1.7 dB) and become almost negligible at 10.5 μm. The reason for these discrepancies is explained in terms of additional scattering losses due to the inner metallic surface roughness, which are inversely proportional to the wavelength squared [14, 15].

2. Theory

Propagation losses in hollow waveguides are highly dependent on the launch conditions. In general, longer focal length lenses excite lower-order modes within the waveguides, decreasing the interaction of the light with the waveguide walls and minimizing the attenuation. In order to quantify this, we assume a perfect Gaussian beam coupled into the waveguide entrance. The spot size $\omega(z)$ can be shown to vary with propagation distance z along the optical axis as [16]:

$$\omega^2(z) = \omega_0^{\,2}\left[1+\left(\frac{z_0}{R}\right)^2\right] \tag{1}$$

where ω_0 is the beam waist and R is the wave front radius. The parameter $z_0 = \pi\omega^2/\lambda$ is the Rayleigh range. According to these expressions, only one parameter is needed to completely specify the waist ω_0 at the focal length of a lens, i.e., the laser beam spot size on the coupling lens.

The theoretical analysis of optical mode structure in dielectric hollow-core waveguide has been described in detail in [17–19]. The fundamental modes are the HE_{nm} hybrid modes, which have a small component of the electric field along the fiber or optic axis and correspond to skew rays (rays that do not cross the fiber axis; rather they travel in a corkscrew or helical paths down the waveguide). The HE_{11} mode is the lowest order mode having a circularly-symmetric, Gaussian spatial profile. When a Gaussian beam is properly focused into a hollow waveguide along the optic axis, only the HE_{1m} modes are excited inside the waveguide. This is a result of the strong dependence of loss on the waveguide mode parameter. The losses of high order modes increase as the square of the mode parameter so even though the guides are multimode, in practice only the lowest order modes propagate. This is particularly true for small-bore (≤ 300 μm) waveguides. In order to theoretically estimate propagation losses L_p of the HCWs we take into account both the power coupling efficiency η_{1m} of the Gaussian incident beam to each HE_{1m} waveguide mode and the attenuation coefficients α_{1m} of the HE_{1m} modes by using the following expression:

$$L_p(dB) = -10Log_{10}\left(\sum_m \eta_{1m} e^{-2\alpha_{1m}L}\right) \tag{2}$$

where L is the length of the HCW. The power coupling efficiency of each HE_{1m} mode can be expressed as the normalized overlap integral between the input Gaussian mode with a beam waist ω_0 at the waveguide entrance, and the HE_{1m} waveguide modes, which can be approximated by zero-order Bessel functions. Hence, the power-coupling coefficient for the various modes is a function of $2\omega_0/d$, i.e., ω_0 divided by the bore radius of the waveguide and so depends on how much the focused beam fills the hollow waveguide. A minimal loss condition is achieved when this ratio is about 0.64 [9]. Hence, an appropriate focal length lens is needed to approximate as much as possible this ratio, in order to optimize the laser beam coupling into the HCW. For a HCW with a bore diameter d = 200 μm, optimal coupling occurs for ω_0 = 64 μm, which for λ = 5 μm corresponds to a numerical aperture $NA = \lambda/(\pi\cdot\omega_0)$ = 0.025. Thus, relatively slow optics provide optimal coupling into the lowest order mode. When faster optics are used (i.e., a smaller beam size that under fills the HCW bore) there will be less coupling into the lowest order mode and more coupling into the higher order modes. On the opposite extreme, if the beam size is bigger than the HCW bore, the coupling efficiency will decrease due to clipping of the beam and the lowest order mode will be preferentially selected. For the attenuation coefficients α_{1m} at each HE_{1m} mode, we used the expression derived by Miyagi and Kawakami [20]:

$$\alpha_{1m} = \left(\frac{u_{1m}}{2\pi}\right)^2 \frac{\lambda^2}{a^3}\left(\frac{n}{n^2-k^2}\right)\left\{\frac{1}{2}\left[1+\frac{n_d^2}{\left(n_d^2-1\right)^{1/2}}\right]^2\right\} \tag{3}$$

where n and k are the real and imaginary parts of the complex index of the metallic (typically Ag) layer, η_{1m} is the *mth* root of the zero-order Bessel function and a is the HCW bore radius. For the wavelength dependence of n, k and n_d we used relations reported in [21].

3. Experimental setup

In this work, we employed two HCWs with metallic (Ag)/dielectric (AgI) circular cross-section internal coatings, a bore size of d = 200 µm, and of 15 cm and 50 cm. Fabrication of the HCWs is accomplished using a wet chemistry process developed by Harrington et al. [5, 6]. It consists of depositing a reflective silver (Ag) layer followed by a dielectric silver iodide (AgI) layer inside a HCW tube. The glass tubing does not influence the optical properties of the HCW, but simply provides a smooth surface on which the coatings are applied. An external protective buffer on the outside of the capillary tube helps to shield the glass from scratching. By producing a hollow fiber with a specific dielectric thickness layer, the transmission spectrum of the waveguides can be tailored for different spectral wavelength ranges. The optimal dielectric film that minimizes propagation losses into the fiber for a wavelength of λ = 5 µm is 0.46 µm, assuming that the refractive index n_d of silver iodine at this wavelength is 1.965 [21]. The actual thickness of the AgI layer, calculated from the Fourier transform infrared spectrometer, is about 0.56 µm [9]. Three commercial mid-IR external cavity quantum cascade laser (QCL) sources (Daylight Solutions Inc., San Diego, CA, USA, model #21052-MHF, #21062-MHF, #21106-MHF) were employed to investigated the attenuation of the hollow waveguides, the optical mode profile at the waveguide exit and the influence of the input launch conditions on the beam propagation through the fibers. The laser sources can work in the ranges 5.10-5.34 µm (#21052-MHF); 5.92-6.27 µm (#21062-MHF); 9.94-10.72 µm (#21106-MHF). For each laser source, we study the fiber-output mode profile in all the operating spectral range. In the present work we show results obtained when operating the three QCL sources at the following wavelengths: λ_a = 5.4 µm, λ_b = 6.2 µm and λ_c = 10.5 µm. Under these conditions, the emitted optical powers were 115 mW (λ_a), 80 mW (λ_b), and 56 mW (λ_c). The couplings between the QCLs and the hollow waveguide have been realized by using the experimental scheme shown in Fig. 1. A coupling lens with a diameter of 1/2" and attached to a translation mount was used to focus the collimated laser beam into the HCW entrance. The HCW was held in a kinematic mount, which allowed for tilt adjustments of the position of the HCW entrance with respect to the focused laser beam. In order to record the mode profile in the far field, a pyrocamera (Pyrocam III, Ophir Spiricon) with pixel sizes of 0.085 x 0.085 mm was mounted at distances ≥ 2.5 cm from the HCW output.

#225874 - $15.00 USD Received 28 Oct 2014; revised 11 Dec 2014; accepted 16 Dec 2014; published 5 Jan 2015

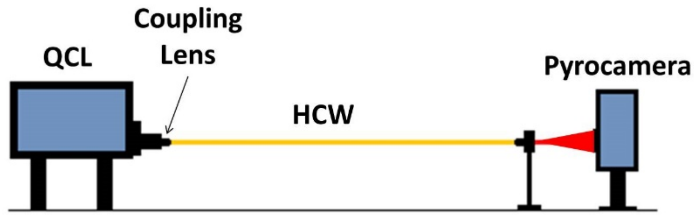

Fig. 1. A schematic of the experimental setup. The laser beam is focused into the HCW entrance using a coupling lens. The beam profile at the waveguide exit is acquired with an infrared pyrocamera. QCL –Quantum Cascade Laser; HCW – Hollow-Core Waveguide.

4. Output beam profiles

Figures 2(a) and 2(b) show the far field spatial intensity distributions of the λ_a-QCL and λ_c-QCL sources measured when shining the beams on to the detector sensitive area (without the presence of the HCW). The 2D profiles of the input beams resemble Gaussian beam power distributions.

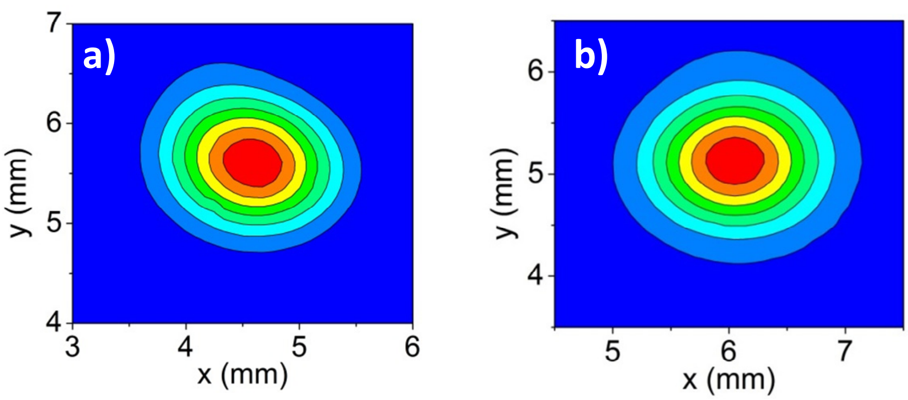

Fig. 2. Far field spatial intensity distribution of λ_a-QCL (a) and λ_c-QCL (b). The beam profile was measured directly by shining the QCL output on to the detector, positioned at ~2.5 cm from the QCL.

For each QCL source, the output beam divergence was measured acquiring the far field profile at two different distances from the laser output and by measuring the radial distances at which the light intensity drops to $1/e^2$ of its maximum central value. For the λ_a-QCL a beam radius R_0 = 1.18 mm and a diffraction-limited beam divergence angle of ϑ_A = 2.9 mrad were measured. In a similar way, we measured R_0 = 1.33 mm and ϑ_B = 3.1 mrad for λ_b-QCL and R_0 = 1.2 mm and ϑ_C = 5.6 mrad for λ_c-QCL.

To investigate the influence of the input launch conditions on the beam propagation through the HCW, we employed three different coupling lenses, with focal length *f* of 25 mm, 50 mm and 76 mm. In Table 1 are reported the $2\omega_0/d$ ratios calculated at λ_a and λ_b by using Eq. (1), where d = 200 µm. In each case, the alignment was optimized by maximizing the HCW output power, by adjusting the coupling lens position and the waveguide entrance tip/tilt mounting. Based on our calculations, the optimum coupling conditions can be obtained using a lens with f = 50 mm, both for λ_a-QCL and λ_b-QCL, with a focused beam collimated down to a ~70 µm spot radius at the HCW entrance.

#225874 - $15.00 USD Received 28 Oct 2014; revised 11 Dec 2014; accepted 16 Dec 2014; published 5 Jan 2015

Table 1. Ratios $2\omega_0/d$ calculated for three coupling lenses for both the λ_a-QCL (beam radius of 1.18 mm) and the λ_b-QCL (beam radius of 1.33 mm).

	λ_a	λ_b
f (mm)	**$2\omega_0/d$**	**$2\omega_0/d$**
25	0.36	0.37
50	0.72	0.74
76	1.10	0.113

Figures 3(a)-3(f) show the far field spatial intensity distribution obtained in a straight line condition (i.e. with no HCW bending) for λ_a-QCL at the exit of a 15 cm [Figs. 3(a)-3(c)] and 50 cm [Figs. 3(d)-3(f)] long HCW, by using coupling lenses with focal length of $f = 25$ mm [Fig. 3(a) and Fig. 3(d)], $f = 50$ mm [Fig. 3(b) and Fig. 3(e)] and $f = 76$ mm [Fig. 3(c) and Fig. 3(f)].

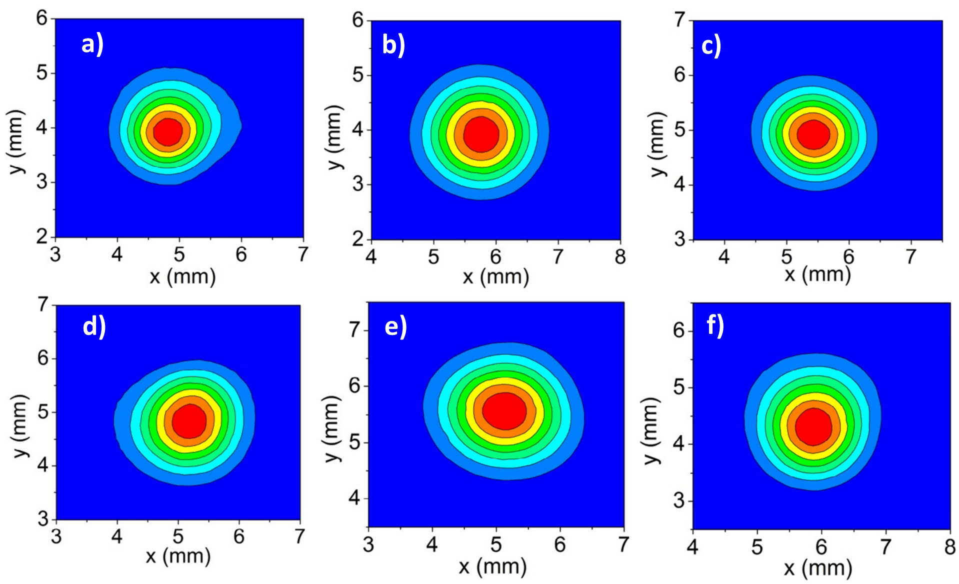

Fig. 3. Far field spatial intensity distribution of λ_a-QCL upon exiting at 15 cm-long [(a), (b) and (c)] and 50 cm-long [(d), (e) and (f)] HCW, employing coupling lenses with focal lengths: f = 25 mm [(a), (d)], f = 50 mm [(b), (e)] and f = 76 mm [(c), (f)]. The beam profiles have been obtained with the experimental scheme illustrated in Fig. 1. The distance between the fiber output and the pyrocamera has been fixed to 2.5 cm.

The 2-D far field acquisitions demonstrate that HCWs with bore sizes of 200 μm allow single-mode propagation of laser beam at $\lambda = 5.4$ μm, with both the 15 cm and 50 cm long fibers. In addition, even though the coupling conditions are significantly different, the modal purity is good, resulting in a beam shape matched to the hybrid HE_{11} mode in almost all investigated configurations. We also verified that the single mode HCW operation is preserved during the entire laser source operating range, down to 5.1 μm.

The output divergence angle is the result of both the diffraction of light leaving the waveguide and the beam quality. It depends critically on both the nature of the optical mode propagating through the HCW, and the bore diameter. In principle, the output beam divergence can provide an indication of the number of high-order modes propagating in the HCW. The HE_{11} mode will couple to free-space modes with a beam divergence θ given by [5]:

#225874 - $15.00 USD Received 28 Oct 2014; revised 11 Dec 2014; accepted 16 Dec 2014; published 5 Jan 2015

$$\theta = \frac{u_{11}\lambda}{2\pi a} \tag{4}$$

From our data, for the best coupling conditions f = 50 mm, we calculate for λ_a (λ_b) a divergence of 25.0 mrad (26.5 mrad) in good agreement with the expected theoretical value of 20.6 mrad (23.9 mrad), calculated by using Eq. (4) with u_{11} = 2.4048. The quality of the output beam can be expressed by the ratio r of the measured beam divergence angle and the calculated one. We estimated r = 1.19 for λ_a and r = 1.11 for λ_b, indicating a good beam quality and the possibility to be re-focused to a tight spot.

5. Propagation losses

Absolute values of the losses of the excited mode in the HCW were determined by measuring the optical power at the waveguide entrance and the optical power at the output-end of the HCW by using a mid-IR power meter. Figures 4(a)-4(d) show the propagation losses α of 15 cm [Figs. 4(a) and 4(c)] and 50 cm [Figs. 4(b) and 4(d)]-long HCWs measured as a function of the ratio $2\omega_0/d$, using λ_a-QCL [Figs. 4(a) and 4(b)] and λ_b-QCL [Figs. 4(c) and 4(d)] at different coupling conditions. Figure 4 includes, for comparison, the theoretical losses α_{1m} for these waveguides calculated at λ_a [Figs. 4(a) and 4(b)] and λ_b [Figs. 4(c) and 4(d)] using Eqs. (2) and (3), assuming that the HE_{11} and higher-order modes up to m = 5 propagate.

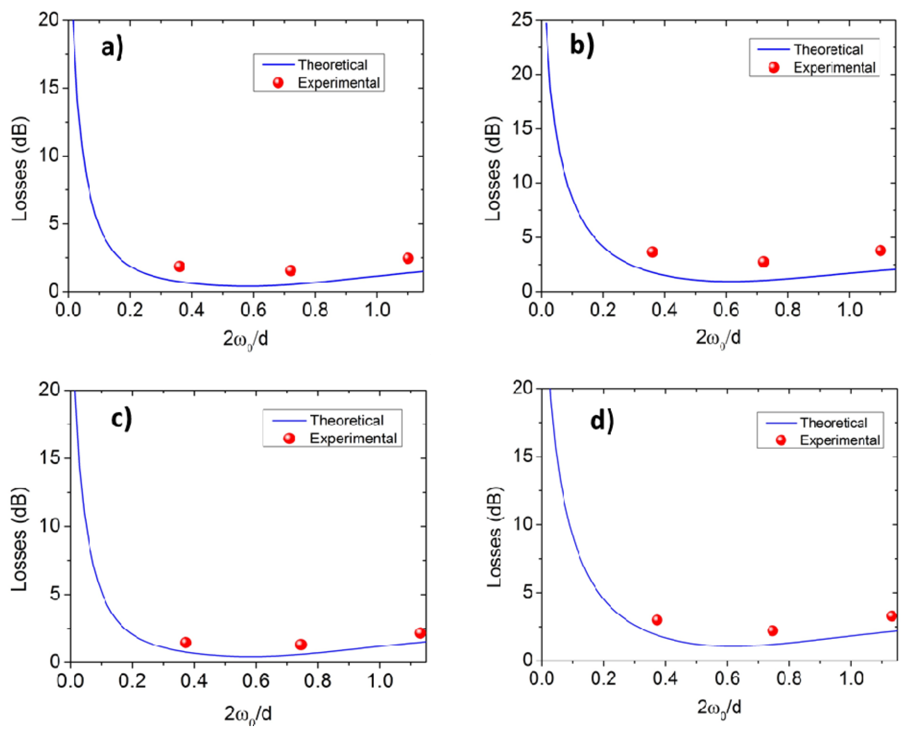

Fig. 4. Total losses (dots) calculated from the ratio between input/output power values of λ_a-QCL [(a) and (b)] and λ_b-QCL [(c) and (d)] at the 15 cm-long [(a) and (c)] and 50 cm-long [(b) and (d)] hollow waveguides exit/entrance. The solid lines are theoretical losses α_{1m} calculated using Eq. (2) and (3).

The experimental losses follow the trend predicted by the theoretical model of Miyagi [20]. However, they result higher than the calculated α_{1m} values. This discrepancy between theoretical and experimental values increases for the longer HCWs. A possible explanation for the observation of losses higher than expected can be the presence of additional scattering

#225874 - $15.00 USD Received 28 Oct 2014; revised 11 Dec 2014; accepted 16 Dec 2014; published 5 Jan 2015

losses, not predicted by theory and due to roughness of the HCW internal reflective coating layers. Matsuura et al. [22], using a ray-optics approach, demonstrated that these scattering losses decrease with wavelength as $1/\lambda^2$. To confirm this, we coupled the 200 µm-HCWs with the λ_c-QCL emitting at 10.5 µm by using the same experimental setup reported in Fig. 1 and three different lenses with focal length *f* of 25 mm, 40 mm and 50 mm. In Table 2 are reported the calculated $2\omega_0/d$ ratios assuming a λ_c-QCL beam diameter of 2.4 mm.

Table 2. Ratios $2\omega_0/d$ calculated for three different coupling lenses and λ_c-QCL.

	λ_c
f (mm)	$2\omega_0/d$
25	0.69
40	1.11
50	1.39

The optimal coupling condition should be ensured by using the lens with *f* = 25 mm. Figure 5(a) depicts a representative far-field spatial intensity distribution of λ_c-QCL at the exit of 15 cm-long HCW, measured 2.5 cm away from the HCW output and employing a coupling lens with *f* = 25 mm. Figure 5(b) shows the measured and theoretical straight losses at different coupling conditions as a function of $2\omega_0/d$ ratio.

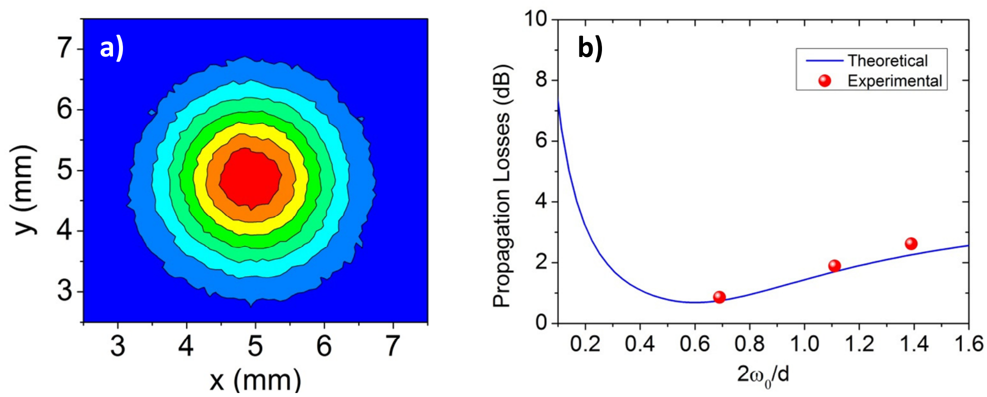

Fig. 5. (a) Far field spatial intensity distribution of λ_c-QCL upon exiting a 15 cm long HCW by using the coupling lens with f = 25 mm. (b) Experimental losses (dots) as a function of $2\omega_0/d$ ratio. The solid line represents the theoretical losses trend calculated by using Eqs. (2) and (3) for λ_c.

Single-mode propagation has been obtained for all three lenses employed and in the entire QCL operating range. At 10.5 um we obtained a good agreement between the losses predicted by the theory and the experimental results, demonstrating that the contribution due to scattering losses results is almost negligible for this longer wavelength. In addition, this result confirms that our HCWs have a nearly ideal structure of the glass and perfect circular uniformity of the cross section [22, 23].

In Fig. 6, the discrepancy α - α_{1m} between the measured losses and the theoretical values was plotted as a function of $1/\lambda^2$ for a 50 cm-long HWC at λ_a, λ_b and λ_c when $2\omega_0/d$ equals 0.72, 0.74 and 0.69 (see Table 1 and Table 2), i.e., the best achievable conditions in terms of output mode quality.

The results show an almost linear behavior, as predicted by Matsuura et al. [21], thereby supporting the notion that an additional contribution to the total losses originates from light scattering due to surface roughness of the inner HCW metallic layer.

#225874 - $15.00 USD Received 28 Oct 2014; revised 11 Dec 2014; accepted 16 Dec 2014; published 5 Jan 2015

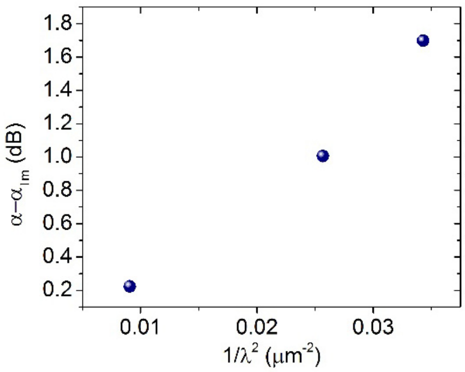

Fig. 6. Differences between theoretical and experimental losses measured for λ_a, λ_b and λ_c for a 50 cm-long HWC plotted as a function of $1/\lambda^2$.

6. Bending losses

An additional loss for HCWs is due to the waveguide bending. The dependence of such losses from HCW curving radius has been investigated for different metallic, and single-layer dielectric coated HCWs with bore size > 300 µm [14, 15]. In Fig. 7(a) we show the bending losses measured at $\lambda = 5.2$ µm, for the 200 µm-bore diameter HCW of length $L = 50$ cm and employing a coupling lens with $f = 50$ mm.

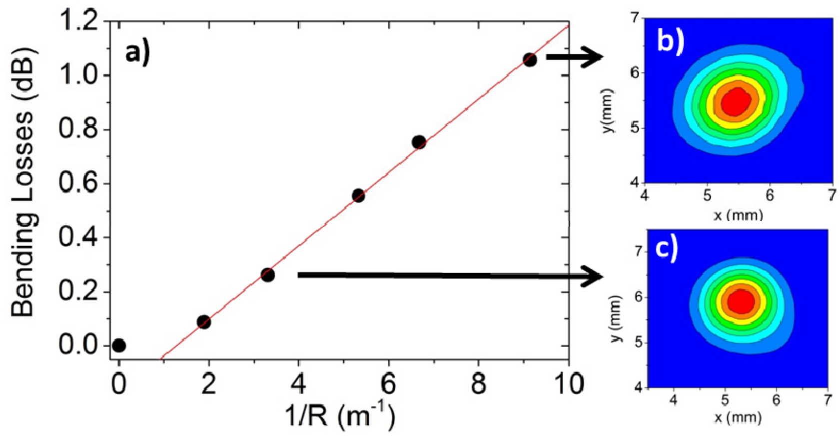

Fig. 7. (a) Bending losses (dots) for 50cm-long HCW measured by using λ_a-QCL and the coupling lens with f = 50 mm. Solid line is the best linear fit of the data below the critical radius $R_c = 1.15$ m. (b) Mode profile at the HCW exit bent at a radius of curvature of 0.111 m. (c) Mode profile at the HCW exit bent at a radius of curvature of 0.302 m. The corresponding data points are marked by arrows.

Figures 7(b) and 7(c) show two representative measured profiles of the 50cm-long HCW bent to a 0.111 m radius and to a 0.302 m radius, respectively. For these measurements, the input and output ends of the guides are kept straight, and the bent portion of waveguide was kept constant. The data in Fig. 7(a) show that below a critical radius (R_c = 1.15 m), the bending losses increase linearly with the reciprocal of the radius of curvature. The solid line in Fig. 7(a) is the best linear fit to the experimental data. The linear trend is characteristics of HCWs and the magnitude of this loss depends largely on the quality of the inner surface [24].

#225874 - $15.00 USD Received 28 Oct 2014; revised 11 Dec 2014; accepted 16 Dec 2014; published 5 Jan 2015

7. Conclusions

Up to now, mid-IR single mode operation was demonstrated at $\lambda \leq 5.5$ µm with solid core fibers [11] or $\lambda \geq 7.6$ µm with HCWs [13]. In this work, we demonstrated single-mode propagation in the spectral range 5.1-10.5 µm using a HCW with bore size of 200 µm. In this way, single-mode operation now cover all the mid-IR spectral range. The waveguide optical properties depend on the laser beam launch conditions into the fiber, and propagation losses have been predicted by using fundamental waveguide theory. An additional contribution to the waveguide losses was measured and attributed to scattering losses, i.e. the interaction of light with the imperfect inner surface of the metallic layer in the hollow waveguide. Our study shows that these losses scale roughly as $1/\lambda^2$ and become almost negligible at 10.5 µm. Bending losses have been measured as a function of the radius of fiber curvature and a linear dependence was observed below a critical radius. Our measurements demonstrate that it is possible to generate a single-mode HE_{11} output profile even if the guide is bent up to $1/R$ ~10 m^{-1}. As a final remark, consider that the input beam quality determines the minimum fiber length providing single mode operation, so the achievement of single mode propagation with the 15-cm long fiber is also due to the excellent beam quality of the employed QCLs.

Acknowledgments

The authors from Dipartimento Interateneo di Fisica di Bari acknowledge financial support from three Italian research projects: PON01 02238, PON02 00675 and PON02 00576.

#225874 - $15.00 USD Received 28 Oct 2014; revised 11 Dec 2014; accepted 16 Dec 2014; published 5 Jan 2015